Clinical Trial/Experimental Study

Medicine®

OPEN

Antilung cancer effect of ergosterol and cisplatin-loaded liposomes modified with cyclic arginine-glycine-aspartic acid and octa-arginine peptides

Meijia Wu, MS[a], Ting Huang, MS[b], Juan Wang, MS[a], Ping Chen, MS[a], Wanwan Mi, MS[a], Yuanyuan Ying, MS[a], Hangli Wang, MS[a], Dandan Zhao, MS[c], Shengwu Huang, MB[a,*]

Abstract

Background: Lung cancer is one of the most important diseases threatening human health, and targeted therapy has become the main research direction. This work, therefore, aimed to develop cyclic arginine-glycine-aspartic (RGD) and octa-arginine (R8) peptide-modified ergosterol (ERG)-combined cisplatin (diamminedichloridoplatinum(II) [DDP]) liposomes (LIP) as a drug delivery system.

Methods: Soybean phospholipids (SPC) and cholesterol (Chol) were selected to prepare different LIPs: ERG-loaded LIP (ERG-LIP), DDP and ERG-LIP (DDP/ERG-LIP), R8 peptide-modified DDP and ERG-LIP (R8-DDP/ERG-LIP), and cyclic RGD and R8-DDP/ERG-LIP (RGD/R8-DDP/ERG-LIP). The quality, tumor sphere penetrating ability, in vitro cellular uptake, mechanism of cellular uptake, and in vitro cytotoxicity of RGD/R8-DDP/ERG-LIP were evaluated.

Results: The LIP quality evaluation revealed that RGD/R8-DDP/ERG-LIP is round with a double-layer structure. The average particle size, dispersion coefficient of the polydispersity index (PDI), and zeta potential of RGD/R8-DDP/ERG-LIP were 155.2 ± 8.7 nm, 0.102, and 4.74 ± 0.7 mV, respectively. Furthermore, the LIPs were stable in the serum, and obviously inhibited the growth of A549 lung cancer cells with RGD/R8-DDP/ERG-LIP exhibiting the strongest inhibitory effect. The highest cellular uptake rate, which was at 4 hours, was exhibited by RGD/R8-DDP/ERG-LIP in a concentration-dependent manner.

Conclusion: The results showed that LIP uptake by A549 cells was mainly by the clathrin-mediated endocytosis pathway (chlorpromazine). The results also suggest that RGD/R8-DDP/ERG-LIP might be a promising drug delivery system to improve antilung cancer drug effect and tumor-targeting in vitro.

Abbreviations: ANOVA = analysis of variance, BFGF = basic fibroblast growth factor, Chol = cholesterol, DAPI = 4′,6-diamidino-2-phenylindole, DDP = cisplatin (diamminedichloridoplatinum(II)), DL = drug load, DSPE = 1,2-Distearoyl-sn-glycero-3-phosphoethanolamine, EE = encapsulation efficienc, EGF = epidermal growth factor, EPR = enhanced permeability and retention, ERG = ergosterol, FITC = fluorescein isothiocyanate, LIP = liposomes, MTT = 3-(4,5-dimethylthiazol-2-yl)-2,5-diphenyltetrazolium bromide, NSCLC = nonsmall cell lung cancer, OD = absorbance value (optical density), PBS = phosphate-buffered saline, PDI = polydispersity index, PEG = poly ethylene glycol, R8 = octa-arginine, RGD = cyclic arginine-glycine-aspartic, RPMI = Roswell Park Memorial Institute, SD = standard deviation, SPC = soybean phospholipids.

Keywords: A549 cells, cancer, cellular uptake, cisplatin, ergosterol, liposome, quality evaluation, targeting

1. Introduction

Malignant tumor is one of the most important diseases threatening human health. The wide gap between the vessel wall, incomplete structure, and lack of lymphatic drainage in the tumor tissue cause large molecular substances and nano-drug delivery systems in the tumor site to exhibit a strong enhanced permeability and retention (EPR) effect.[1–3] Studies have exploited this feature of the tumor tissue by encapsulating drugs in microparticle carriers, which effectively target the tumor site to induce therapeutic effect via the EPR effect.[4–6]

Recently, medicinal fungi have shown promise in the treatment of nonsmall cell lung cancer (NSCLC) with a reliable curative effect.[7–9] Ergosterol (ERG) is one of the triterpene constituents of Taiwan's unique *Antrodia camphorata* formulation. The antitumor activity of ERG was first reported in 1994.[10] In 2003, a study showed that ERG in yeast has a strong inhibitory effect on the growth of breast cancer cells in vitro.[11] Lin et al[12] found that ERG combined with amphotericin B can effectively induce necrosis of human hepatoma cells. Currently, the antilung cancer effect of ERG has not been reported. Cisplatin (DDP) is the most commonly used drug to treat lung cancer; a combination of DDP and ERG can be used to achieve an improved therapeutic effect.

Liposomes have good biocompatibility and targeting and can be used as a delivery vehicle for various types of drugs.[13–16] Furthermore, liposomes can simultaneously load lipophilic (ERG) and hydrophilic (DDP) drugs.[17–19] Liposomes are easily eliminated from the body, and polyethylene glycol (PEG)-modified

Editor: Miao Liu.

The study was supported by the National Natural Science Foundation of China (No. 81473361).

The authors have no conflicts of interest to disclose.

Supplemental Digital Content is available for this article.

[a] College of Pharmaceutical Science, Zhejiang Chinese Medical University, [b] General Surgical Department, Hangzhou Red Cross Hospital, [c] Pharmacy Department, Hangzhou Zhongxing Hospital, Hangzhou, Zhejiang, China.

[*] Correspondence: Shengwu Huang, College of Pharmaceutical Science, Zhejiang Chinese Medical University, Hangzhou, Zhejiang, 311402, China (e-mail: hsw55@163.com).

Medicine (2018) 97:33(e11916)

Received: 18 April 2018 / Accepted: 20 July 2018

http://dx.doi.org/10.1097/MD.0000000000011916

liposomes can increase the circulation time in vivo, leading to a high accumulation in the tumor tissue.[20,21]

The transmembrane peptides can efficiently transport proteins, nucleic acids, and nanomaterials into the cell.[22] Typical transmembrane peptides include TAT (AYGRKKRRQRRR) and octa-arginine (R8, RRRRRRRR). However, the membrane peptides generally lack tissue selectivity. In addition, TAT and R8 are positively charged and can combine with the plasma proteins to reduce their stability. These properties significantly limit the applicability of transmembrane peptides in vivo.[23] Integrin is a class of cell adhesion receptor molecule that is widely expressed on the surface of nuclear cells. Integrin αvβ3 is highly expressed in glioma, melanoma, and lung cancer cells, as well as tumor-associated endothelial cells. Therefore, integrin αvβ3 is frequently used for targeting specific tumors.[24,25] A study showed that tripeptide sequences of arginine-glycine-aspartic acid (Arg-Gly-Asp, RGD) can specifically recognize integrins containing αv subunit with high affinity.[26] The introduction of cyclic RGD peptide effectively avoids the drawbacks of the R8 peptide.

In this study, an ERG-loaded liposome (ERG-LIP) was prepared by the film dispersion method, and the entrapment efficiency of ERG was used as the evaluation index. Subsequently, DDP was combined with the ERG liposome, and DDP was encapsulated by the ammonium chloride gradient method. The entrapment efficiency of DDP was used as the evaluation index. 1,2-Distearoyl-sn-glycero-3-phosphoethanolamine-conjugated PEG3400 (DSPE-PEG3400-c, RGDfk) and DSPE-PEG1000-R8 were embedded into DDP and ERG-LIP (DDP/ERG-LIP) membranes by the post-insertion method. Further, cyclic RGD and R8 peptide-modified ERG-DDP-LIP (RGD/R8-DDP/ERG-LIP) was prepared.

In this study, RGD/R8-DDP/ERG-LIP was characterized for morphology, particle size distribution, and zeta potential. The serum stability, tumor penetrability, in vitro cytotoxicity, uptake by A549, and the mechanism of uptake were also investigated.

2. Methods

2.1. Materials and cells

A549 human NSCLC cells were purchased from the Shanghai Institutes for Biological Sciences, Chinese Academy of Sciences. The reference standards of ERG and DDP were purchased from the National Institutes for Food and Drug Control. Furthermore, ERG, DDP, and fluorescein isothiocyanate (FITC) were purchased from Sigma-Aldrich Corporation, St. Louis. Soybean phospholipids were purchased from the Shanghai Aladdin Biochemical Technology Co., Ltd, Shanghai, China Injections of high-purity cholesterol was purchased from the Shanghai Yiweite Pharmaceutical Technology Co., Ltd, Shanghai, China DSPE-PEG3400-COOH and DSPE-PEG1000-COOH were purchased from the US Nanocs Inc., New York. The polycarbonate track-etched membrane was purchased from Whatman, UK. PEG400 used was of pharmaceutical grade, and it was purchased from the American DOW Chemical company. All other chemicals were of reagent grade.

The study protocol was approved by the institutional review board of Zhejiang Chinese Medical University. All of the procedures were performed in accordance with the Declaration of Helsinki and relevant policies in China.

2.2. Preparation of RGD/R8-DDP/ERG-LIP

First, we used a membrane dispersion method to prepare the ERG-LIP.[27] Soybean phospholipids (SPC), cholesterol (Chole), and ERG were completely dissolved in chloroform, and then placed in a rotary evaporator at 40°C water bath, and 300 mmol L^{-1} ammonium chloride was added to the horizontal rocking bed at 25°C for 30 minutes. After hydration, the membranes were removed by ultrasound. The probe was subjected to ultrasonography for 20 minutes. We used 0.8, 0.45, and 0.22 μm filters for filtration. Finally, the sample was extruded through a polycarbonate membrane (0.1 μm) at high pressure. As DDP is weakly alkaline, we used the ammonium chloride gradient method to prepare the DDP/ERG-LIP. To the prepared ERG-LIP solution, DDP solution was added and incubated at 50°C for 10 minutes. Subsequently, using the post-insertion method,[28] R8-DDP/ERG-LIP, RGD-DDP/ERG-LIP, and RGD/R8-DDP/ERG-LIP were prepared by incubating DDP/ERG-LIP with the modified peptides for 1 hour in a 55°C water bath. In addition, the FITC-labeled LIP was prepared by adding appropriate amount of FITC methanol solution to the lipid material to form a thin film by rotary evaporation.

2.3. Characterization of RGD/R8-DDP/ERG-LIP

The characteristic shape of DDP/ERG-LIP, RGD-DDP/ERG-LIP, R8-DDP/ERG-LIP, and RGD/R8-DDP/ERG-LIP were determined by transmission electron microscopy (TEM). The particle distribution and zeta potential of samples diluted 20 times were measured using a laser particle size analyzer/zeta potentiometer. The serum stability of DDP/ERG-LIP and RGD/R8-DDP/ERG-LIP was investigated to simulate in vivo conditions.

2.4. Tumor sphere penetrability

In vivo tumor tissue is composed of multiple layers of cells, and therefore, we examined the tumor sphere penetrability of RGD/R8-DDP/ERG-LIP under different pH conditions to simulate the in vivo microenvironment. Furthermore, 20 μg mL^{-1} B27 serum-free medium, 20 ng mL^{-1} epidermal growth factor (EGF), and basic fibroblast growth factor (bFGF) were added to the culture medium, half of which was changed every 3 days. A mixed solution of RGD/R8-DDP/ERG-LIP and culture medium at pH 6.0 and 7.4 was added to six-well plates and incubated with tumor spheres for 2 h. The tumor spheres were aspirated, collected by centrifugation, rinsed thrice with phosphate-buffered saline (PBS), and then Lyso-Tracker Red was added to a final concentration of 1 μg mL^{-1}, followed by incubation for 30 minutes. The culture medium was discarded, and then the cells were rinsed thrice with PBS, and then fixed with 4% paraformaldehyde for 30 minutes. Subsequently, the supernatant was discarded after centrifugation, the cells were rinsed thrice with PBS, stained with 1 μg mL^{-1} 4′,6-diamidino-2-phenylindole (DAPI) solution for 5 minutes, the supernatant was discarded, and the spheres were rinsed thrice with PBS. The tumor spheres were plated on polylysine-treated slides and blocked with 10% glycerol-PBS. The penetrability of RGD/R8-DDP/ERG-LIP was observed using an FV1000 confocal laser scanning microscope.

2.5. In vitro cellular uptake

The cellular uptake rate of liposomes at different concentrations was determined at varying times by flow cytometry with laser confocal microscopy. Quantitatively prepared FITC-labeled DDP/ERG-LIP, RGD-DDP/ERG-LIP, R8-DDP/ERG-LIP, and RGD/R8-DDP/ERG-LIP samples were mixed with Roswell Park Memorial Institute (RPMI) 1640 culture medium at pH 7.4. A549 cells were seeded in six-well plates containing medium with

10% serum and incubated at 37°C in a 5% CO_2 incubator until cell fusion reached approximately 80%. After aspirating the culture medium, DDP/ERG-LIP, RGD-DDP/ERG-LIP, R8-DDP/ERG-LIP, and RGD/R8-DDP/ERG-LIP with different concentrations were added, followed by incubation for 2 hours, and then the culture medium was aspirated, the cells were rinsed thrice with PBS, and digested with trypsin. After centrifugation, the cells were resuspended in 0.5 mL PBS. The uptake intensity of RGD/R8-DDP/ERG-LIP at different concentrations was determined by BD flow cytometry. The same method was repeated at different time points: 0, 30, 60, 90, 120, 150, 180, 210, and 240 minutes. The uptake intensity of RGD/R8-DDP/ERG-LIP at different time points was determined by BD flow cytometry.

A549 cells were seeded in small, specific dishes of diameter of 35 mm containing medium with 10% serum for laser confocal microscopy and incubated in 37°C in a 5% CO_2 incubator until cell fusion reached approximately 80%. After aspirating the culture medium, 128-fold diluted DDP/ERG-LIP, RGD-DDP/ERG-LIP, R8-DDP/ERG-LIP, and RGD/R8-DDP/ERG-LIP samples were added. After 2 hours, the culture medium was aspirated, the cells were rinsed thrice with PBS, and then Lyso-Tracker Red was added to a final concentration of 1 $\mu g\,mL^{-1}$. After incubating the cells for 30 min, the culture medium was discarded, the cells were rinsed thrice with PBS, 4% paraformaldehyde was added, and incubated for 30 min. Subsequently, the cells were rinsed thrice with PBS and stained with 1 $\mu g\,mL^{-1}$ DAPI solution for 5 minutes. Finally, the cells were rinsed thrice with PBS and the infiltrating cells were collected with 600 μL of PBS. The uptake of DDP/ERG-LIP, RGD-DDP/ERG-LIP, R8-DDP/ERG-LIP, and RGD/R8-DDP/ERG-LIP was observed using an FV1000 laser confocal microscope.

2.6. Mechanism of cellular uptake

A549 cells were seeded in six-well plates containing medium with 10% serum and incubated at 37°C in a 5% CO_2 incubator until cell fusion reached approximately 80%. Subsequently, 500 $\mu g\,mL^{-1}$ of cellular uptake inhibitors chlorpromazine hydrochloride (clathrin-mediated endocytosis pathway inhibitor), clozapine (caveolin-mediated endocytosis pathway inhibitor), colchicine (macropinocytosis inhibitor), and sodium azide (energy-dependent endocytosis pathway inhibitor) were incubated with A549 cells for 30 minutes, followed by the addition of RGD/R8-DDP/ERG-LIP. After 2 hours, the culture medium was aspirated, the cells were rinsed thrice with PBS, and digested with trypsin. After centrifugation, the cells were resuspended in 0.5 mL of PBS, and the uptake of RGD/R8-DDP/ERG-LIP by A549 cells was detected in the presence of various inhibitors by flow cytometry. Furthermore, the uptake mechanism was investigated.

2.7. In vitro cytotoxicity assay

The cytotoxicity of DDP/ERG-LIP, RGD-DDP/ERG-LIP, R8-DDP/ERG-LIP, and RGD/R8-DDP/ERG-LIP was tested on A549 cells by the 3-(4,5-dimethylthiazol-2-yl)-2,5-diphenyltetrazolium bromide (MTT) assay. Each well of the 96-well plates containing medium with 10% serum was seeded with 10^4 cells in the logarithmic growth phase and incubated at 37°C in a 5% CO_2 incubator. When the cells had fused to 80%, they were treated with various concentrations of DDP/ERG-LIP, RGD-DDP/ERG-LIP, R8-DDP/ERG-LIP, and RGD/R8-DDP/ERG-LIP. Five wells were allocated for each concentration, and the MTT assay was performed at 2 and 24 hours after treatment by the addition of 5 $mg\,mL^{-1}$ MTT solution to each well, followed by incubation for 4 hours at 37°C in a 5% CO_2 incubator. The absorbance value (optical density [OD]) of each well was measured at 492 nm using a microplate reader.

2.8. Statistical analyses

All experiments were performed in triplicates, and the data are expressed as mean ± standard deviation (SD). The statistical analysis of the differences between treatments was performed by the student's *t*-test for pairs of groups and one-way analysis of variance (ANOVA) for multiple groups. All statistical analyses were carried out using the statistical package for the social sciences (SPSS) software (v17.0, Chicago, IL). Furthermore, the results with P values $< .05$ and $< .01$ were considered significant and very significant, respectively.

3. Results

3.1. Preparation of RGD/R8-DDP/ERG-LIP

Figure 1 is a schematic diagram of the synthesis of various LIPs. The conditions for the optimal preparation of ERG-LIP were: SPC and Chol molar ratio, 5:1; ERG drug load (DL), 10%; and probe ultrasound time, 20 minutes. The percent DL (DL%) and the encapsulation efficiency (EE%) of ERG were 10 ± 1.26% and 90.49 ± 1.98%, respectively.

The conditions for the optimal preparation of DDP/ERG-LIP were: DDP, 0.150 $mg\,mL^{-1}$; incubation temperature, and 50°C, and incubation time, 10 minutes. The DL% and EE% of DDP were 2.44 ± 0.54% and 52.24 ± 1.83%, respectively.

DDP and ERG were loaded in the internal aqueous phase and lipid bilayer of liposomes, respectively. Based on that of DDP/ERG-LIP, R8-DDP/ERG-LIP was prepared with SPC, Chole, and DSPE-PEG1000-R8 at a molar ratio of 5:1:0.07. RGD-DDP/ERG-LIP was prepared with SPC, Chole, and DSPE-PEG3400-c(RGDfk) at a molar ratio of 5:1:0.07. Further, RGD/R8-DDP/ERG-LIP was prepared using SPC, Chole, DSPE-PEG1000-R8, and DSPE-PEG3400-c(RGDfk) at a molar ratio of 5:1:0.07:0.07.

3.2. Characterization of RGD/R8-DDP/ERG-LIP

RGD/R8-DDP/ERG-LIP was obtained as a milky white solid with uniform color. The results of microscopy are presented in Figure 2A. Morphologically, the LIPs were round, with a double-layer structure, and uniform particle size distribution. The average particle size, polydispersity index (PDI), and zeta potential of DDP/ERG-LIP were 153.4 ± 5.3 nm, 0.156, and −10.9 ± 0.4 mV, respectively, whereas, the corresponding values for RGD-DDP/ERG-LIP were 156.7 ± 7.5 nm, 0.164 (< 0.3), and −1.29 ± 0.2 mV, respectively. The average particle size, PDI, and zeta potential of R8-DDP/ERG-LIP were 154.3 ± 9.8 nm, 0.178 (< 0.3), and 0.661 ± 0.08 mV, respectively, whereas, those of RGD/R8-DDP/ERG-LIP were 155.2 ± 8.7 nm, 0.102 (< 0.3), and 4.74 ± 0.7 mV, respectively (Fig. 2B and C). The results showed that the particle size distribution of each liposome was concentrated. To investigate the stability of the LIPs in a simulated in vivo environment, their serum stability was determined. The LIPs were incubated with fetal bovine serum for 0.5, 1, 2, 4, 8 and 24 hours and the particle size and zeta potential were measured to investigate their serum stability. Fig. 2D shows that the particle size of the LIPs was approximately

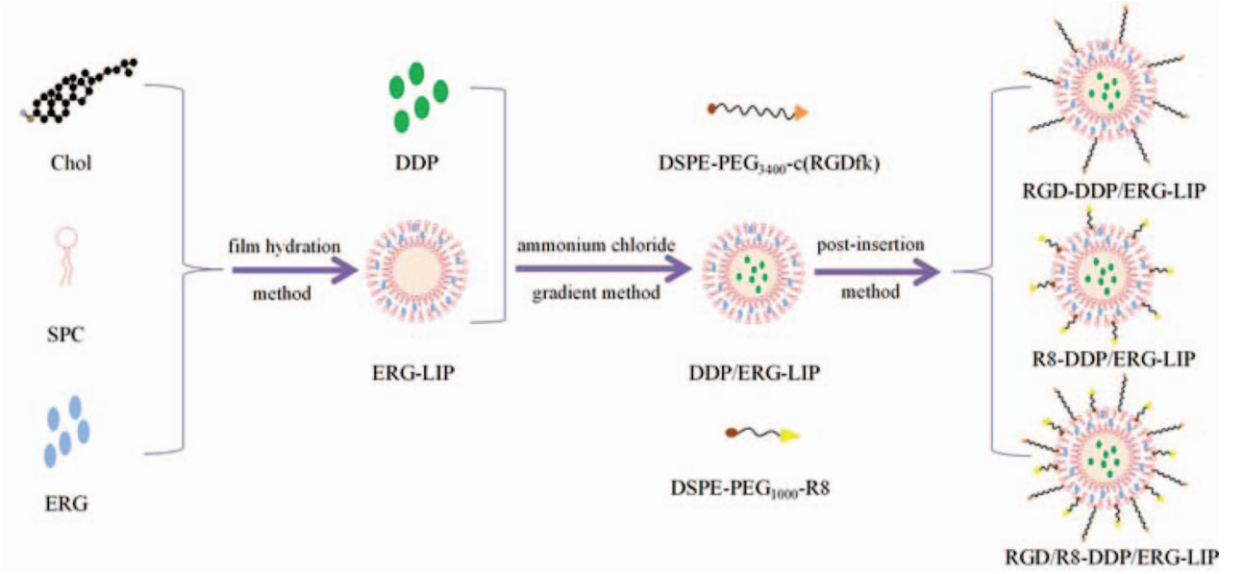

Figure 1. Schematic representation of the synthesis of various liposomes (LIPs). LIPs = liposomes.

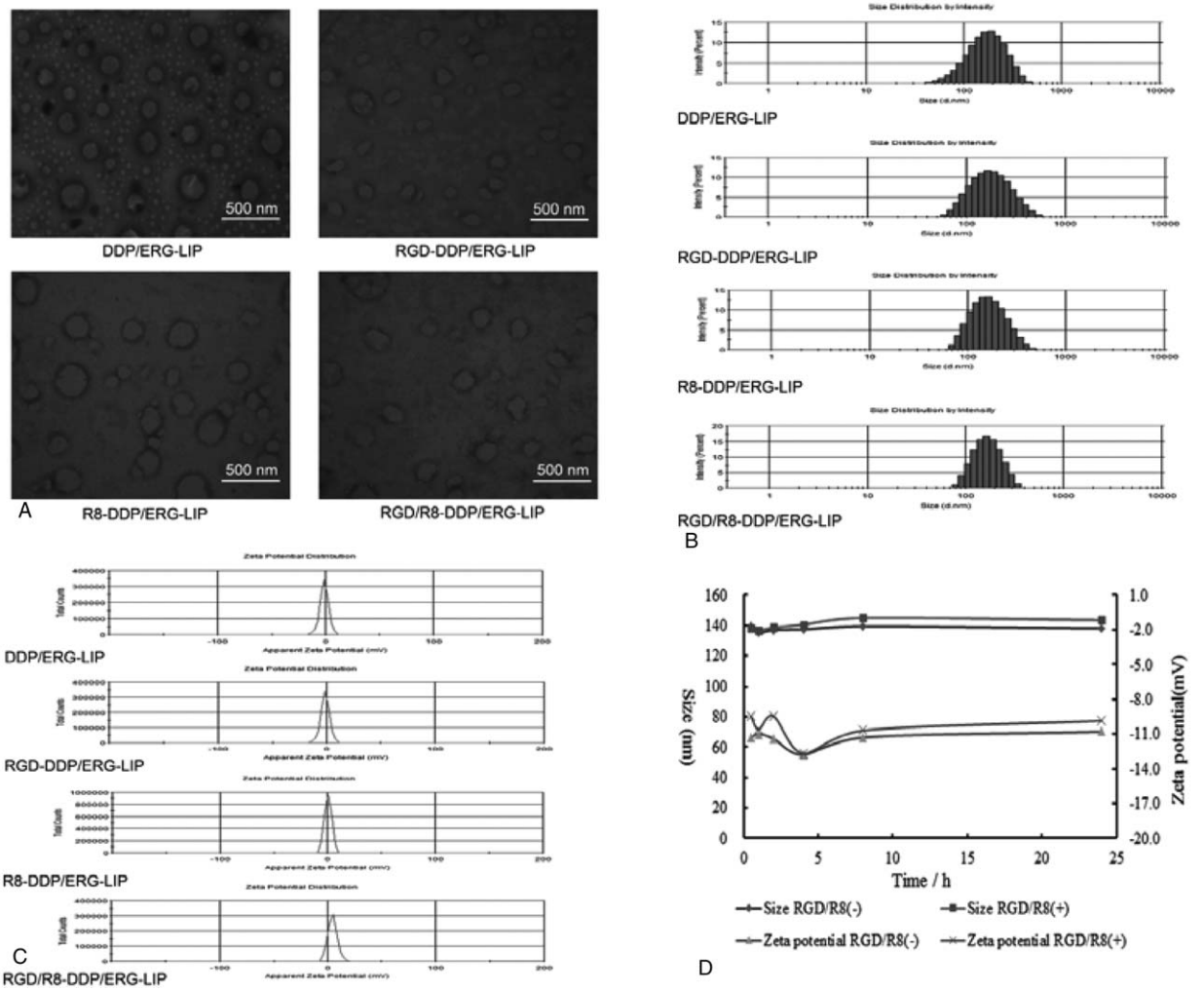

Figure 2. Characterization of liposomes (LIPs). (A) Transmission electron microscopic (TEM) image of LIPs. (B). Size distribution of LIPs. (C) Zeta potential of LIPs. (D) Serological stability of LIPs. The LIPs were incubated with fetal bovine serum for 0.5, 1, 2, 4, 8, and 24 hours. LIPs = liposomes, TEM = transmission electron microscopic.

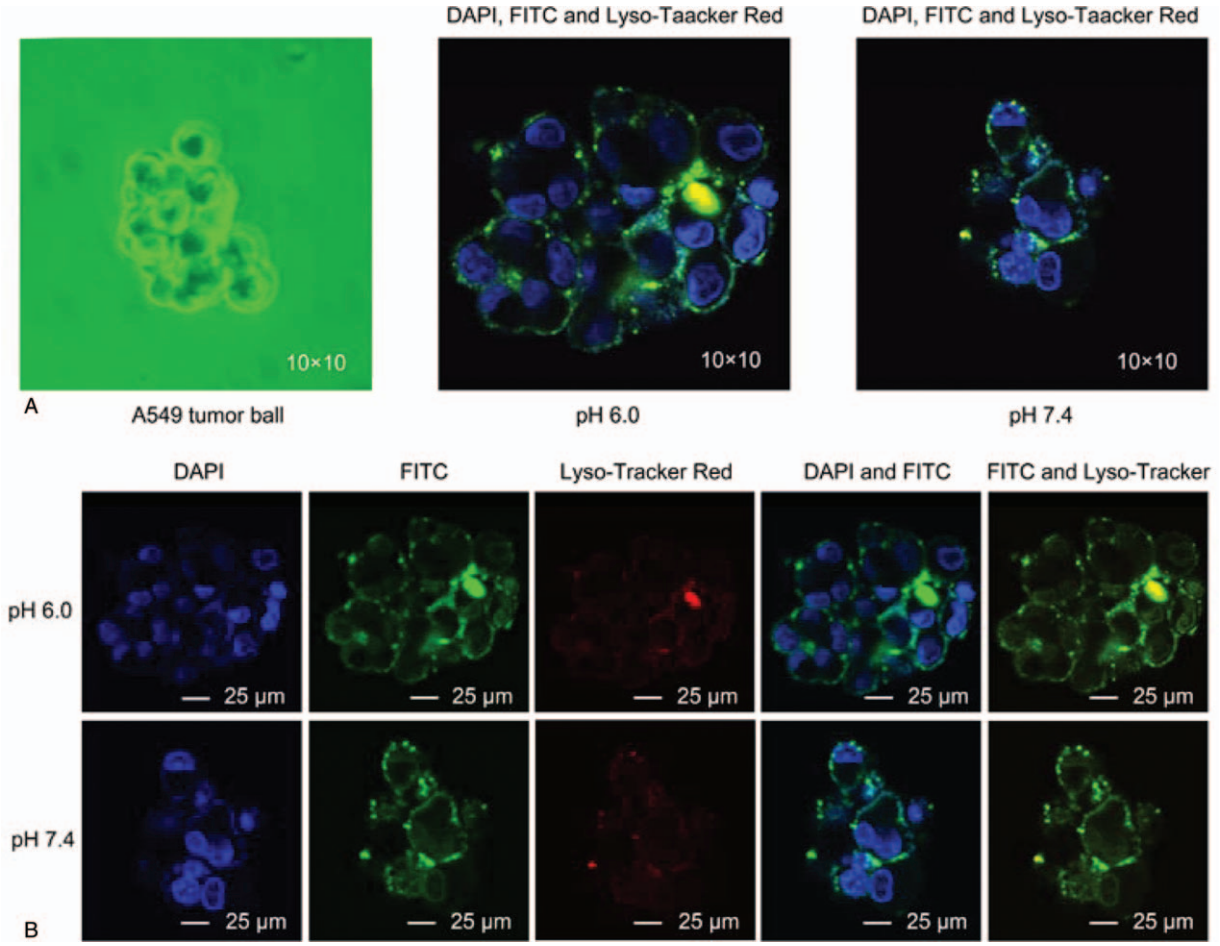

Figure 3. Confocal microscopy imaging results. (A) Schematic representation of the fusion of cyclic arginine-glycine-aspartic (RGD) and octa-arginine (R8) peptide-modified ergosterol (ERG)-combined cisplatin (diamminedichloridoplatinum(II) [DDP]) targeting liposome (LIP, RGD/R8-DDP/ERG-LIP) with A549 tumor cells under different pH conditions. (B) Confocal imaging of co-localized RGD/R8-DDP/ERG-LIP, cell nuclei, and lysosomes under different pH conditions. The cell nuclei were stained with nuclear-specific dye 4′,6-diamidino-2-phenylindole (DAPI), RGD/R8-DDP/ERG-LIP was labeled with fluorescein isothiocyanate (FITC), and lysosomes were labeled with Lyso-Tracker Red (blue, green, and red fluorescence, respectively). DAPI = 4′,6- diamidino-2-phenylindole, DDP = cisplatin (diamminedichloridoplatinum(II)), ERG = ergosterol , FITC = fluorescein isothiocyanate, LIPs = liposomes.

140 nm at different time points and that the LIPs remained stable. The results indicate that RGD/R8-DDP/ERG-LIP had good serum stability.

3.3. RGD/R8-DDP/ERG-LIP has enhanced tumor cell penetration

The pH of RGD/R8-DDP/ERG-LIP determined using an acidity meter was 6.64. Figure 3 shows that the penetrability of the tumor sphere was significantly pH-dependent. The treatment with RGD/R8-DDP/ERG-LIP for 2 hours significantly enhanced the tumor cell penetration at pH 6.0 compared with that at pH 7.4. Furthermore, RGD/R8-DDP/ERG-LIP and the lysosomes were markedly co-localized in treated cells. The color of the lysosomes changed from red to orange, indicating that RGD/R8-DDP/ERG-LIPs were specifically distributed in lysosomes during cell incubation.

3.4. In vitro cellular uptake of the prepared LIPs is affected by LIP concentrations and incubation times

The cellular uptake rate of LIPs was determined by flow cytometry and observed by laser confocal microscopy at different LIP concentrations and uptake times. The results shown in Figure 4A indicate that the uptake fluorescent intensity of RGD/R8-DDP/ERG-LIP was significantly higher than that of both DDP/ERG-LIP and RGD-DDP/ERG-LIP when the concentration of ERG + DDP was $1.09 \pm 1.08\,\mu g\,mL^{-1}$ ($P < .01$). Furthermore, the uptake fluorescent intensity of RGD/R8-DDP/ERG-LIP was significantly higher than that of DDP/ERG-LIP when the concentration of ERG + DDP was $2.19 + 2.16\,\mu g\,mL^{-1}$ and $1.46 + 1.44\,\mu g\,mL^{-1}$ ($P < .01$). Figure 4B shows that the uptake rate of RGD/R8-DDP/ERG-LIP at all other time points was significantly lower than that at 4 hours ($P < .01$). The results of the confocal laser scanning microscopy were consistent with the flow cytometry data. As shown in Figure 4C, the FITC fluorescence intensity of RGD/R8-DDP/ERG-LIP was higher than that of DDP/ERG-LIP, R8-DDP/ERG-LIP, and RGD-DDP/ERG-LIP.

3.5. Cellular uptake of the prepared LIPs occurs via various routes

The LIP uptake rate of each group is shown in Figure 5A. The results showed that when the concentration was $40\,\mu g\,mL^{-1}$, the 4 cellular uptake inhibitors could significantly reduce the uptake

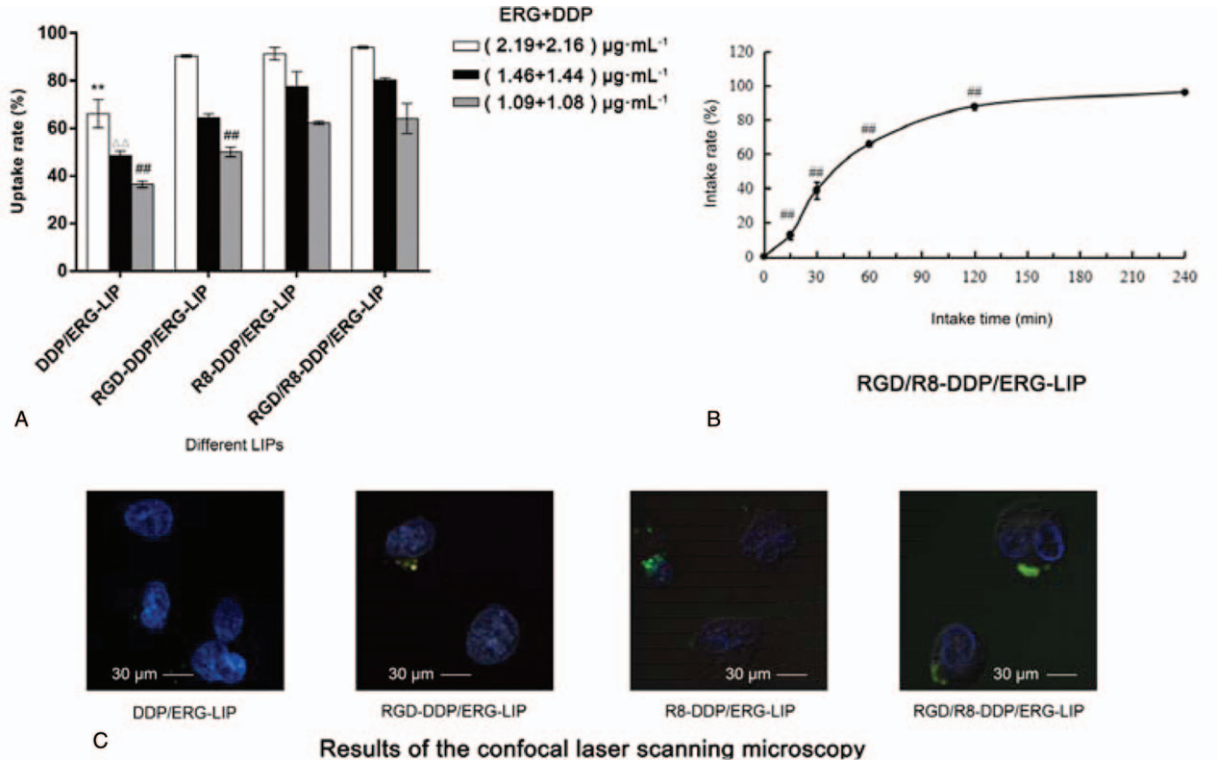

Figure 4. In vitro cellular uptake. (A). Cellular uptake of liposomes (LIPs) at different concentrations. $^{**}P < .01$, compared with cyclic arginine-glycine-aspartic (RGD) and octaarginine (R8) peptide-modified ergosterol (ERG)-combined cisplatin (diamminedichloridoplatinum(II) [DDP]) targeting liposome (RGD/R8-DDP/ERG-LIP, (2.19 + 2.16 μg mL^{-1}); $^{\Delta\Delta}P < .01$, compared with RGD/R8-DDP/ERG-LIP (1.46 + 1.44 μg mL^{-1}); and $^{\#\#}P < .01$, compared with RGD/R8-DDP/ERG-LIP (1.09 + 1.08 μg mL^{-1}) (n = 3). (B) Cellular uptake of RGD/R8-DDP/ERG-LIP at different times. $^{\#\#}P < .01$ (n = 3), compared with cell uptake time of 240 minutes. (C) Cellular uptake was observed by confocal laser scanning microscopy. DDP = cisplatin (diamminedichloridoplatinum(II)), ERG = ergosterol , LIPs = liposomes, RGD = cyclic arginine-glycine-aspartic.

rate of RGD/R8-DDP/ERG-LIP compared with that of the negative control group. Among them, chlorpromazine hydrochloride presented the highest inhibition rate on liposome uptake (down to 40%). The high concentration of inhibitors used might have inhibited cell proliferation, resulting in changes in the cell membrane permeability, which likely affected the uptake rate. To eliminate this interference, the MTT test was performed using various concentrations of uptake inhibitors (Fig. 5B). The results showed that chlorpromazine hydrochloride and clozapine at a concentration of 250 and 100 μg mL^{-1} potently inhibited cell proliferation, whereas the inhibition of various other groups treated with different concentrations was low. The inhibitors at a concentration of 40 μg mL^{-1} did not inhibit cell proliferation, and therefore, antiproliferation effect had no role in the uptake of LIP by A549 cells. Therefore, when comparing the data in Fig. 5A, the concentration of inhibitors (40 μg mL^{-1}) resulting in

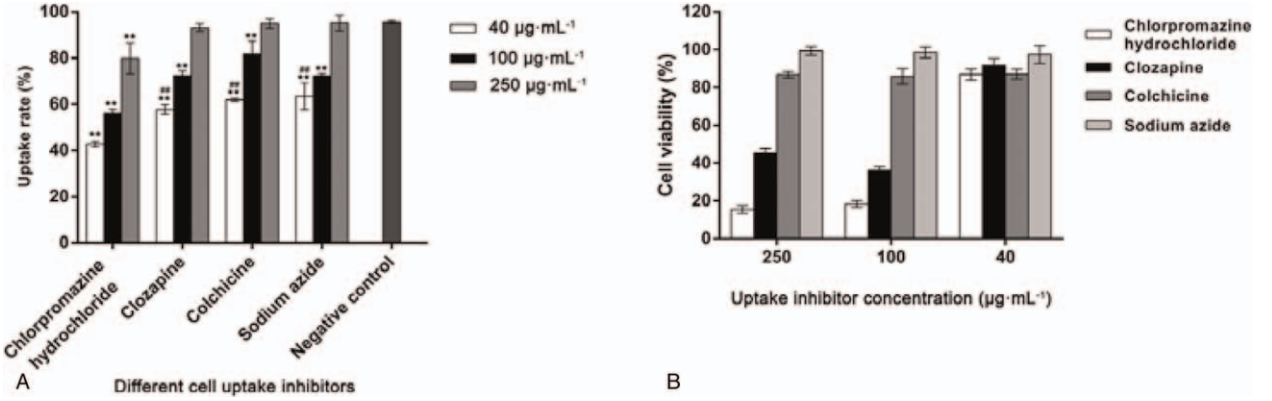

Figure 5. Mechanism of cellular uptake. (A) Flow cytometry results with different cellular uptake inhibitors. $^{**}P < .01$ (n = 3), compared with negative control. Inhibitor concentration, 40 μg mL^{-1}; $^{\#\#}P < .01$ (n = 3), compared with chlorpromazine hydrochloride. (B) In vitro cytotoxicity of different cellular uptake inhibitors (incubation time 30 minutes).

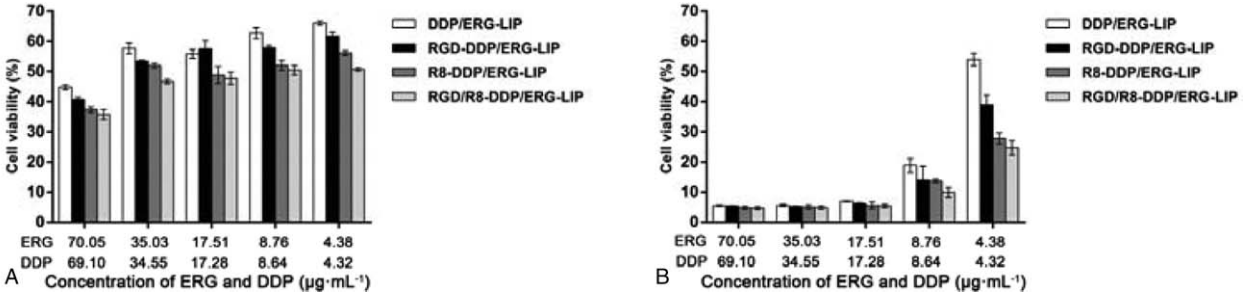

Figure 6. In vitro cytotoxicity assay. In vitro cytotoxicity of liposomes (LIPs) at (a) 2 hours and (b) 24 hours. LIPs = liposomes.

a high cell viability was selected as the reference to identify the uptake mechanism that was dominant. Based on the above results, RGD/R8-DDP/ERG-LIP can be introduced into the cell via a variety of routes.

3.6. R8-DDP/ERG-LIP and RGD/R8-DDP/ERG-LIP have high antiproliferation activity

Following a 2-h treatment, the tumor cell proliferation inhibition rate of R8-DDP/ERG-LIP and RGD/R8-DDP/ERG-LIP was higher than those of DDP/ERG-LIP and RGD-DDP/ERG-LIP when the concentration of ERG + DDP was 70.05 + 69.10, 35.03 + 34.55, 17.51 + 17.28, 8.76 + 8.64, and 4.38 + 4.32 $\mu g\,mL^{-1}$ (Fig. 6A). When the time was prolonged to 24 hours, the inhibition rate of each group showed almost no difference when the concentration of ERG + DDP was 70.05 + 69.10, 35.03 + 34.55, and 17.51 + 17.28 $\mu g\,mL^{-1}$, which was above 90% (Fig. 6B). When the concentration of ERG + DDP was 8.76 + 8.64 and 4.38 + 4.32 $\mu g\,mL^{-1}$, the inhibition rate was the same as that at 2 hours. The results showed that the transmembrane peptide R8 efficiently mediated the release of ERG and DDP by co-modified LIPs into cells, thus achieving a high proliferation inhibition rate.

4. Discussion

Lung cancer is one of the most malignant tumors with the highest morbidity and mortality worldwide, and NSCLC is the most common subtype.[29] Owing to their strong anticancer activity, platinum drugs have become the most important class of drugs for the treatment of malignant tumor.[30] Statistics indicate that 70%–80% of the drugs used for single combination chemotherapy of malignant tumors are platinum based.[31] Although platinum-based anticancer drugs have achieved great success, there are many obstacles to their clinical applications, such as low targeting ability, low side effect threshold, and drug resistance.[32] Furthermore, we found that the alcohol extracts of *Antrodia camphorata* showed good inhibitory effects on the proliferation of A549 cells [Supplementary Material: Figure S1, http://links.lww.com/MD/C405]. The alcohol extracts were separated to identify the components and their effects. The results showed that the ERG component strongly inhibited the proliferation of A549 cells. Therefore, we considered that the combination of DDP and ERG would exhibit enhanced antiproliferative effects. We then formulated a targeting LIP drug delivery system with cyclic RGD and R8 peptide modifications to achieve collaborative delivery and reduce the toxicity of DDP.

The in vitro serum stability test showed that RGD/R8-DDP/ERG-LIP was stable for 24 hours. The mixture of LIP and serum exhibited good stability, mainly because the PEG content shielded the positive charge of membrane peptide R8, reduced the plasma protein level, and improved the stability. These findings lay a foundation for further research on in vivo and in vitro drug targeting. Furthermore, the stability of LIP requires follow-up investigations for longer time points to ensure the quality of the prepared LIP.

Tumor tissues consist of multilayer cells in vivo, and to simulate this microenvironment to evaluate the effect of the formulations, the penetrability of RGD/R8-DDP/ERG-LIP across tumor spheres was investigated in different pH media. The tumor sites are generally acidic, and the results showed that the penetrability was significantly enhanced at pH 6 (Fig. 3), which further indicated the adequate targeting of RGD/R8-DDP/ERG-LIP. Moreover, the staining analysis revealed that lysosomes were co-localized with RGD/R8-DDP/ERG-LIP, which confirmed the hypothesis that the drug is released in these digestive organelles following the degradation of lipid matrix.

In addition, transmembrane peptide-mediated LIP delivery has a variety of endocytosis pathways including energy-dependent endocytosis, charge-dependent endocytosis, macropinocytosis, clathrin-mediated endocytosis, and caveolin-mediated endocytosis pathways.[33–35] However, sodium azide and colchicine induced no change in cell viability (Fig. 5B) at concentrations of 40, 100, and 250 $\mu g\,mL^{-1}$, but the liposome uptake still increased with concentration. Therefore, considering the data in Fig. 5A, cell uptake inhibitors were incubated for 30 minutes and RGD/R8-DDP/ERG-LIP was incubated for 2 hours. However, the cell uptake inhibitor was incubated for 30 minutes in the MTT assay (Fig. 5B). We conjecture that the proliferation inhibition effect of sodium azide and colchicine at 30 minutes was not obvious, but after 2 hours of incubation (although there was RGD/R8-DDP/ERG-LIP), the inhibition of cell proliferation increased. Alternatively, RGD/R8-DDP/ERG-LIP, sodium azide, and colchicine might affect cell uptake via another mechanism, which needs further exploration.

The aim of this study was to develop a cyclic RGD/R8-DDP/ERG-LIP drug delivery system with a strong inhibitory effect on tumor cell proliferation, cell uptake abilities, and tumor tissue penetrability. The results suggest that RGD/R8-DDP/ERG-LIP might be a promising drug delivery system as it exhibited certain degree of in vitro targeting. Furthermore, it can improve antilung cancer effect and tumor targeting properties of drugs in vitro.

Acknowledgements

We would like to thank Editage (www.editage.cn) for English language editing.

Author contributions

Conceptualization: Meijia Wu, Ting Huang, Wanwan Mi.
Data curation: Meijia Wu, Juan Wang.
Formal analysis: Juan Wang, Yuanyuan Ying.
Funding acquisition: Shengwu Huang.
Investigation: Ting Huang, Ping Chen.
Methodology: Shengwu Huang.
Project administration: Shengwu Huang.
Resources: Ting Huang, Shengwu Huang.
Software: Hangli Wang.
Supervision: Shengwu Huang.
Validation: Ping Chen, Wanwan Mi.
Visualization: Yuanyuan Ying.
Writing – original draft: Meijia Wu, Dandan Zhao.
Writing – review & editing: Meijia Wu, Hangli Wang, Shengwu Huang.

References

[1] Mikada M, Sukhbaatar A, Miura Y, et al. Evaluation of the enhanced permeability and retention effect in the early stages of lymph node metastasis. Cancer Sci 2017;108:846–52.
[2] Saisyo A, Nakamura H, Fang J, et al. pH-sensitive polymeric cisplatin-ion complex with styrene-maleic acid copolymer exhibits tumor-selective drug delivery and antitumor activity as a result of the enhanced permeability and retention effect. Colloids Surfaces B Biointerfaces 2016;138:128–37.
[3] Nichols JW, You HB. EPR: Evidence and fallacy. J Control Release 2014;190:451–64.
[4] Zhao T, Huang G, Li Y, et al. A Transistor-like pH nanoprobe for tumour detection and image-guided surgery. Nat Biomed Eng 2016;1:0006.
[5] Maeda H, Nakamura H, Fang J. The EPR effect for macromolecular drug delivery to solid tumors: Improvement of tumor uptake, lowering of systemic toxicity, and distinct tumor imaging in vivo. Adv Drug Deliv Rev 2013;65:71–9.
[6] Nakamura Y, Ai M, Choyke PL, et al. Nano-drug delivery: is the enhanced permeability and retention (EPR) effect sufficient for curing cancer? Bioconjug Chem 2016;27:2225–38.
[7] Liu X, Wu X, Ma Y, et al. Endophytic fungi from mangrove inhibit lung cancer cell growth and angiogenesis in vitro. Oncol Rep 2017;37:1793–803.
[8] Majeed S, Abdullah MS, Dash GK, et al. Biochemical synthesis of silver nanoprticles using filamentous fungi Penicillium decumbens (MTCC-2494) and its efficacy against A-549 lung cancer cell line. Chinese J Nat Med 2016;14:615–20.
[9] Zhang J, Lai Z, Huang W, et al. Apicidin inhibited proliferation and invasion and induced apoptosis via mitochondrial pathway in non-small cell lung cancer GLC-82 cells. Anticancer Agents Med Chem 2017;17:1–1.
[10] Yasukawa K, Aoki T, Takido M, et al. Inhibitory effects of ergosterol isolated from the edible mushroom Hypsizigus marmoreus on TPA-induced inflammatory ear oedema and tumour promotion in mice. Phytother Res 1994;8:10–3.
[11] Subbiah MT, Abplanalp W. Ergosterol (major sterol of baker's and brewer's yeast extracts) inhibits the growth of human breast cancer cells in vitro and the potential role of its oxidation products. Int J Vitam Nutr Res 2003;73:19–23.
[12] Lin YC, Lee BH, Alagie J, et al. Combination treatment of ergosterol followed by amphotericin B induces necrotic cell death in human hepatocellular carcinoma cells. Oncotarget 2017;8:72727–38.
[13] Zhou G, Li L, Jing X, et al. Redox responsive liposomal nanohybrid cerasomes for intracellular drug delivery. Colloids Surf B Biointerfaces 2016;148:518–25.
[14] Ma M, Lei M, Tan X, et al. Theranostic liposomes containing conjugated polymer dots and doxorubicin for bio-imaging and targeted therapeutic delivery. RSC Adv 2016;6:1945–57.
[15] Wang Y, Wang B, Liao H, et al. Liposomal nanohybrid cerasomes for mitochondria-targeted theranostics. J Mater Chem B 2015;3:7291–9.
[16] Singla AK, Garg A, Aggarwal D. Paclitaxel and its formulations. Int J Pharm 2002;235:179–92.
[17] Poy D, Akbarzadeh A, Ebrahimi SH, et al. Preparation, characterization and cytotoxic effects of liposomal nanoparticles containing cisplatin: an in vitro study. Chem Biol Drug Des 2016;88:568–73.
[18] Shein SA, Kuznetsov II, Abakumova TO, et al. VEGF and VEGFR2-targeted liposomes for cisplatin delivery to glioma cells. Mol Pharm 2016;13:3712–23.
[19] Zhang LJ, Kuang Y, Zhuo RX, et al. Anionic long circulating liposomes for hepatic targeted delivery of cisplatin. J Control Rel 2015;213:e72.
[20] Li SD, Huang L. Stealth nanoparticles: high density but sheddable PEG is a key for tumor targeting. J Control Rel 2010;145:178–81.
[21] Zhang J, Chen Y, Li X, et al. The influence of different long-circulating materials on the pharmacokinetics of liposomal vincristine sulfate. Int J Nanomed 2016;11:4187–97.
[22] Wehland JD, Lygina AS, Kumar P, et al. Role of the transmembrane domain in SNARE protein mediated membrane fusion: peptide nucleic acid/peptide model systems. Mol Biosyst 2016;12:2770–6.
[23] Zhang L, Wang Y, Gao HL, et al. The construction of cell-penetrating peptide R8 and pH sensitive cleavable polyethylene glycols co-modified liposomes. Acta Pharm Sinica 2015;50:760–6.
[24] Hegi ME, Diserens AC, Gorlia T, et al. MGMT gene silencing and benefit from temozolomide in glioblastoma. N Engl J Med 2005;352:997–1003.
[25] Ying X, Wen H, Lu WL, et al. Dual-targeting daunorubicin liposomes improve the therapeutic efficacy of brain glioma in animals. J Control Rel 2010;141:183–92.
[26] Khalil IA, Kogure K, Futaki S, et al. Octaarginine-modified liposomes: enhanced cellular uptake and controlled intracellular trafficking. Int J Pharm 2008;354:39–48.
[27] De KB, Gerritsen WJ, Oerlemans A, et al. Polyene antibiotic-sterol interactions in membranes of Acholesplasma laidlawii cells and lecithin liposomes. II. Temperature dependence of the polyene antibiotic-sterol complex formation. Biochim Biophys Acta 1974;339:44–56.
[28] Iden DL, Allen TM. In vitro and in vivo comparison of immunoliposomes made by conventional coupling techniques with those made by a new post-insertion approach. Biochim Biophys Acta 2001;1513:207–16.
[29] Siva S, Callahan J, Kron T, et al. A prospective observational study of Gallium-68 ventilation and perfusion PET/CT during and after radiotherapy in patients with non-small cell lung cancer. BMC Cancer 2014;14:740.
[30] Dilruba S, Kalayda GV. Platinum-based drugs: past, present and future. Cancer Chemother Pharmacol 2016;77:1103–24.
[31] Buffoni L, Vavalà T, Novello S. Adjuvant therapy of resected non-small cell lung cancer: can we move forward? Curr Treat Options Oncol 2016;17:54.
[32] Gao C, Zhang Y, Chen J, et al. Targeted drug delivery system for platinum-based anticancer drugs. Mini Rev Med Chem 2016;16:872–91.
[33] Calero M, Chiappi M, LazaroCarrillo A, et al. Characterization of interaction of magnetic nanoparticles with breast cancer cells. J Nanobiotechnol 2015;13:1–5.
[34] Kim HR, Gil S, Andrieux K, et al. Low-density lipoprotein receptor-mediated endocytosis of PEGylated nanoparticles in rat brain endothelial cells. Cell Mol Life Sci 2007;64:356–64.
[35] Kang JH, Jang WY, Ko YT. The effect of surface charges on the cellular uptake of liposomes investigated by live cell imaging. Pharm Res 2017;34:1–4.